
Proceedings Paper:
West, P., Hart, J., Guymer, I. et al. (1 more author) (2016) Development of a laboratory system and 2D routing analysis to determine solute mixing within aquatic vegetation. In: Rowinski, P.M. and Marion, A., (eds.) Hydrodynamic and Mass Transport at Freshwater Aquatic Interfaces. XXXIV International School of Hydraulics, 11-14 May 2015, Żelechów, Poland. GeoPlanet: Earth and Planetary Sciences . Springer , pp. 49-61.

https://doi.org/10.1007/978-3-319-27750-9_5

Development of a laboratory system and 2D routing analysis to determine solute mixing within aquatic vegetation

Patrick West, James Hart, Ian Guymer, and Virginia Stovin[1]

Abstract

A laser induced fluorometry (LIF) system was developed to quantify mixing within spatially variable aquatic vegetation. A comparison is made between intrusive fluorometry techniques and the application of LIF, to quantify mixing in real vegetation in the laboratory setting. LIF provides greater spatial resolution when compared to point fluorometry. Furthermore, LIF is non-intrusive. A two-dimensional routing procedure is used to calculate the longitudinal and transverse velocities and mixing coefficients from a single pulse injection of tracer within a vegetated patch.

1 Introduction

Diffuse, or non-point source, contamination is the most significant contributor to surface water pollution within the UK and Europe (National Audit Office & Environment Agency, 2010). Pond and wetland environments are becoming an increasingly favoured method of providing appropriate pre-treatment before contaminated water enters major watercourses (Kadlec & Wallace, 2009; Serra *et al*. 2004). As well as offering ecological habitat and amenity to local residents, wetland treatment systems present an integrated approach to sustainable water resource management. The presence of vegetation in these systems acts as a habitat for organisms (Taylor *et al*. 1995) and bio-chemical degradation of contaminants (Edgar, 1990; Kadlec and Knight, 1996; Dixon and Florian, 1993; Nixon, 1980). Moreover, vegetation affects the local hydrodynamics and thus the installation's detention characteristics (Nepf, 1999; Nepf *et al*. 2007; Burba *et al*. 1999).

P. West, I. Guymer, J. Hart School of Engineering, Univeristy of Warwick, Coventry CV4 7AL, e-mail: p.west@warwick.ac.uk, e-mail: i.guymer@warwick.ac.uk, e-mail: j.hart@warwick.ac.uk

V. Stovin
Department of Civil and Structural Engineering, The University of Sheffield, Mappin St., Sheffield, S1 3JD, UK.
e-mail: v.stovin@sheffield.ac.uk

The prevalence of controlled laboratory studies (White and Nepf, 2007; Ghisalberti and Nepf, 2005, 2002; Nepf *et al*. 2007; Boxall and Guymer, 2007) has helped to understand the influence of hydrodynamics and channel porosity on detention times and dispersion. Laboratory studies have also proved essential when verifying, often empirical, modelling techniques (Serra *et al*. 2004 Ghisalberti & Nepf, 2005.). From previous laboratory studies there is a paucity of information on the influence of plant species, age and geometry on solute mixing.

Pond systems generally comprise borders and patches of emergent vegetation (e.g. Fig. 1). The lateral heterogeneity in drag caused by these patches influences the velocity field creating a complex, multi-dimensional system (Ghisalberti and Nepf, 2004, 2002; Nepf *et al*. 2007; Nepf and Vivoni, 2000; Murphy *et al*. 2007; White and Nepf, 2007; Rominger and Nepf, 2011). Fig. 1 shows an example of a field trace study in a large treatment pond (Hart *et al*, 2014). The fluorescent dye highlights the spatially variable flow fields around borders and patches of vegetation.

This paper describes the development of a laboratory method and analysis technique as part of a 3 year EPSRC funded grant projects 'Residence Times in Vegetated Stormwater Ponds EP/K024442/1 and EP/K025589/1'. The project aims are to derive an understanding of how the hydraulic residence time of a stormwater pond is affected by the type and spatial distribution of vegetation. The project has 3 core objectives: to produce a CFD model that can predict how vegetation density and spatial distribution affect the pond's flow field, mixing characteristics and residence time distribution; to collect detailed laboratory data to parameterise the CFD model, and to validate the model against a range of field tests on real stormwater ponds.

Fig. 1 Tracer study used for flow visualization in a treatment pond. Image courtesy of Hart *et al*, 2014.

Tests were conducted in full-width artificial vegetation as a controlled case for the development of the technique – with the view to its later application in shear layer systems. The development and calibration of a bespoke laser induced florescence (LIF) system is described, and compared to the point fluorometry technique. In addition, a 2D routing procedure based on the Advection Dispersion Equation is evaluated to obtain the longitudinal and transverse dispersion

coefficients and respective velocities from pulse tracer injection tests within vegetation patches.

1.1 Background

The trace study in Fig. 1, showing the spatially heterogeneous flows common to ponds, exemplifies the motivation to conduct this research. Tracer dye studies are a common tool for elucidating the hydrodynamic properties of a system (Lightbody and Nepf, 2006a; Shucksmith *et al*. 2011; Kashefipour and Falconer, 2002; Deng *et al*. 2001). Mixing in ponds is a complex phenomenon for two reasons. Firstly, the spatial heterogeneity in the flow field, pond geometry and dispersion can make modelling and experimentation difficult. Secondly, the prevalence of low velocities (< 0.1 m/s) also presents a number of experimental difficulties. If we wish to predict the retention characteristics of ponds with live vegetation then a more robust method for quantifying mixing in aquatic vegetation needs to be developed.

Reynolds number in pond and wetland environments can be very low (Nepf, 1999; Serra *et al*. 2004; Nepf *et al*. 1997). Nepf *et al* (1997) and Serra *et al* (2004) recorded stem Reynolds number in the field at $Re < 200$ and $5<Re<20$, respectively. Stem Reynolds number is used as the preferred length scaling in vegetated flow

$$Re_s = \frac{Ud}{\nu} \tag{1}$$

where the preferred length scale is d, the stem diameter, U is the mean streamwise velocity and ν is the kinematic viscosity of water. It follows that flow in these environments can be fully laminar or transitional from laminar to turbulent (Tamura *et al*. 1980; Nepf *et al*. 1997).

In general, the degree of mixing in a system can be described using a dispersion coefficient [m^2s^{-1}]. Historically this has been calculated by observing the temporal or spatial rate of change of variance in the concentration distribution of a tracer (Fischer, 1968). Here, the term *mixing* is used to describe the cumulative effects of all processes that cause a contaminant to spread or dilute. As such, the term mixing aggregates diffusion, shear dispersion, turbulent diffusion and mechanical diffusion into one parameter. The dispersion coefficient, D, is proportional to the spatial rate of change in variance of the concentration distribution. In the x-direction,

$$D_x = \frac{u}{2}\frac{\mathrm{d}\sigma_x^2}{\mathrm{d}x} \tag{2}$$

where σ^2_x is the variance in the tracer cloud at position x.

The dispersion coefficient and travel time in a particular direction can be optimized by performing a routing procedure from the tracer's temporal concentration distribution (TCD) (Boxall, 2000; Boxall and Guymer, 2007). The downstream TCD is fitted by routing the measured upstream profile until the fit between meas-

urement and prediction is maximized. This process used a Gaussian transfer function. It follows that, if a two-dimensional distribution can be obtained, a two-dimensional routing procedure can optimize the longitudinal dispersion and transverse mixing coefficients and their respective velocities (u and v).

A low Reynolds number does not readily permit assumptions and simplifications – such as rapid cross-sectional mixing and a Gaussian transfer function. Research presented here indicates that, under typical flow velocities in ponds, cross-sectional mixing does not occur for a number of metres from the source. This has implications for the experimental techniques and is described below.

Fig. 2 is a schematic of the phenomena shown in Fig. 1. A velocity shear is caused by the drag discontinuity between the free-flow and the vegetation elements (Nepf and Vivoni, 2000; Ghisalberti and Nepf, 2002). The discontinuity in drag leads to the generation of shear layer vortices. White and Nepf (2007) show that the penetration of shear-generated vortices along an emergent vegetation interface is inversely proportional to the vegetation density.

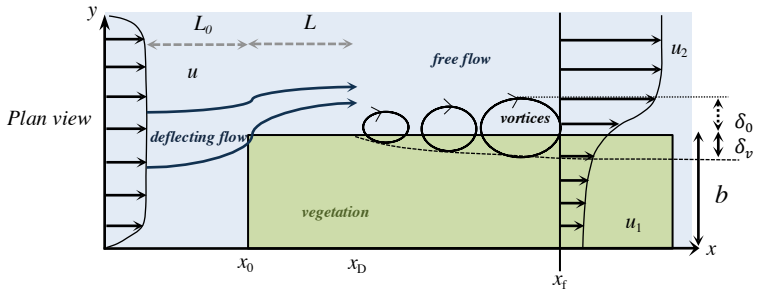

Fig. 2 Vegetated shear layer.

Take the region beyond the extent of the shear layer vortices depicted in Fig. 2. Transverse and/or vertical shear effects are negligible in this fully vegetated emergent region; when compared to stem wake-generated turbulence. Turbulence is therefore found at the scale of the vegetation elements (Lightbody and Nepf, 2006). Thus, the local stem Reynolds number is a preferred method of quantifying turbulence (Serra *et al*, 2004; White and Nepf, 2007; Ghisalberti and Nepf, 2005). Using this preferred scaling, Lightbody and Nepf (2006) show that the transverse mixing coefficient, D_y, in emergent cylinders is dependent on the mean streamwise velocity and the diameter, d, of each element; empirically

$$D_y = 0.17ud \tag{2}$$

Accurate measurement of transverse mixing in real vegetation is lacking. Further, detailed research is lacking for the quantification of mixing processes in and around the partially vegetated/open channel boundary, its bulk effect on wetland retention times and to predict parameters for CFD applications.

1.2 Research Aims

We wish to quantify the mass transport in real vegetated shear layers. Imperative to the observation and quantification of these processes is the successful development of a precise tracer detection system. Mixing in spatially uniform emergent vegetation (fully vegetated) is here used as a test case to develop a measurement process. Rhodamine 6G dye injections are made to observe the spatial and temporal spread of concentration in an array of emergent artificial cylinders and two measurement techniques are compared.

2 Experimental Methods

2.1 Point Probe Fluorometry

Two Rhodamine tracer studies were conducted in a recirculating flat flume at the University of Warwick, UK. The first experiment assessed the feasibility of using point flurometers for measuring spatially variable concentration distributions. Point source pulses of dye were generated in a partially vegetated array of emergent plastic cylinders (Fig. 3). The artificial vegetation was 7 m long with the leading edge 12 m downstream of the inlet to the 24 m long flume. 0.20 m high, 0.004 m diameter plastic straws were arranged in a staggered array spanning 0.3 m of the 0.99 m wide flume.

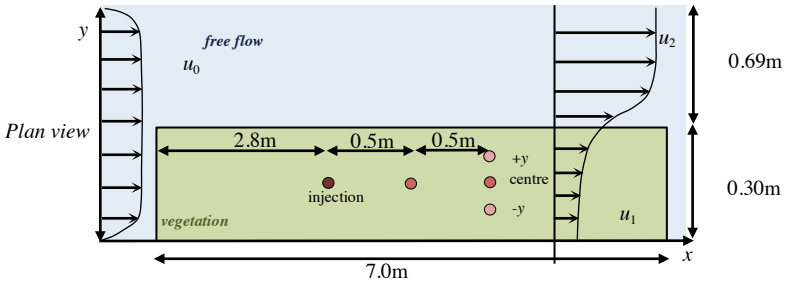

Fig. 3 Fluorometer measurement system. Deviated downstream sites are 0.04 m either side of the centerline.

Dye injections were made 2.8 m downstream of the vegetation leading edge. Ultrasound velocity measurements indicated that this was the location of fully developed flow. A point copper pipe delivered dye to the channel mid-depth and was fed by a constant head tank positioned directly above. Software controlled injections were made via a solenoid valve to enable instantaneous release – providing accuracy in both time of injection and in the mass of tracer. Four discharges (3.0, 5.0, 6.4, 8.4 l/s) were investigated as they produced typical in-vegetation velocities found in ponds, i.e. $u_{1max} \approx 10$ cms^{-1}. In all test cases the mean travel time between longitudinal profiles is used to compute a mean flow velocity.

Tracer pulses were input for 20 seconds. Concentration was measured at 0.5 m and 1.0 m downstream using *Cyclops* fluorometers – positioned in line and at the same depth as the injection point. The low turbulent environment, due to the slow velocities, lead to poor mixing within the trace profile. It was therefore necessary to take up to twenty repeat trials for each test condition. Concentration was measured at 1 Hz to provide adequate temporal resolution. Each pulse was delayed to allow sufficient time for the previous trace to be completely advected through the test section.

The locations of the two downstream fluorometers are shown in Fig. 3. Each test, using the point source injection method, was repeated for these deviated downstream fluorometer locations to observe the lateral spread in concentration distribution. Displacements of y = 4 cm (y+) and y = -4 cm (y-), relative to the injection position, were chosen.

2.2 Laser Induced Fluorometry

The second experiment evaluated Laser Induced Fluorometry (LIF) in its application to record over multiple locations in space – in this case a transverse line. The LIF system was developed to observe spatially variable mixing in the partially vegetated system described in Fig. 3. In this preliminary experiment, LIF was evaluated in the simplified fully vegetated scenario. LIF relies on the same principles employed using the point fluorometer probes. A laser was directed perpendicularly through the flow at the channel mid-depth. As the Rhodamine 6G trace passes through the laser beam the dye absorbs some of the incident light and re-emits it – known as fluorescence. The principle mechanisms of LIF are shown in Fig. 4 indicating the passage of dye through the laser beam. A photo-detector was mounted directly beneath the flow and a wide-angle lens chosen to image the entire beam. Dye concentration is directly proportional to fluorescence intensity and therefore camera pixel intensity. The same laboratory flume depicted in Fig. 3 was also used for this experiment.

Laser attenuation through ~1m of water was significant and laser power was observed to reduce by up to 50%. Further, the laser's attenuation was a function of the local dye concentration. Consider the scenario where intensity is compared from points *A* to *B* (Fig. 4). A weak intensity (and therefore concentration) recorded at *B* could be as a result of two phenomena. Firstly, a comparatively weak concentration is recorded as there is less dye at *B* than *A*. Secondly, the laser beam is attenuated through dye on its propagation to *B* and is weaker, resulting in lower fluorescence. Thus, a simple calibration using the Beer-Lambert Law relating the exponential decay in laser intensity to an attenuation coefficient could not be used. LIF calibration was conducted by recording the change in laser attenuation coefficient as a function of initial laser power. In short, this method considers the power entering a cell and that leaving. If the concentration of the first cell is known, then the concentration of subsequent cells can be determined in a step-by-step effect.

The two LIF windows are shown in Fig. 4. The first window was located 1m downstream of the dye injection point and the second was positioned 1m downstream from that. A 200 mW green laser (λ = 532 nm) was mounted such that it pointed perpendicularly through the flow at a mid-depth of 0.075 m. A small 0.06 m transverse gap within the array was made to accommodate the laser beam and Ultrasound Velocity Profiling (UVP) equipment. Glass windows in the side and bottom of the flume were sealed. A grey-scale camera was mounted underneath each glass window and focused onto the location of the laser beam. The camera shutter-speed was set to maximize the full range of the 8-bit setting for the desired range in trace concentration. Camera images were cropped before saving – to facilitate smooth computer operation – to 20 x 1280 pixels (0.015 m x 0.99 m). Spatial resolution was therefore roughly every millimetre and the resolution in concentration, set by the chosen range in concentration, was 0.2ppb (per pixel intensity). The entire channel system was covered in black-coated wooden paneling to reduce the impact of background ambient light. Discharge was set such that the mean, stream-wise flow velocity, u, within the vegetation was O (1 cms^{-1}). Four discharges were investigated (1.0, 1.8, 2.4, 3.6 l/s); flow depth was maintained at approximately 0.15 m and was measured using a Vernier accurate to 100 microns.

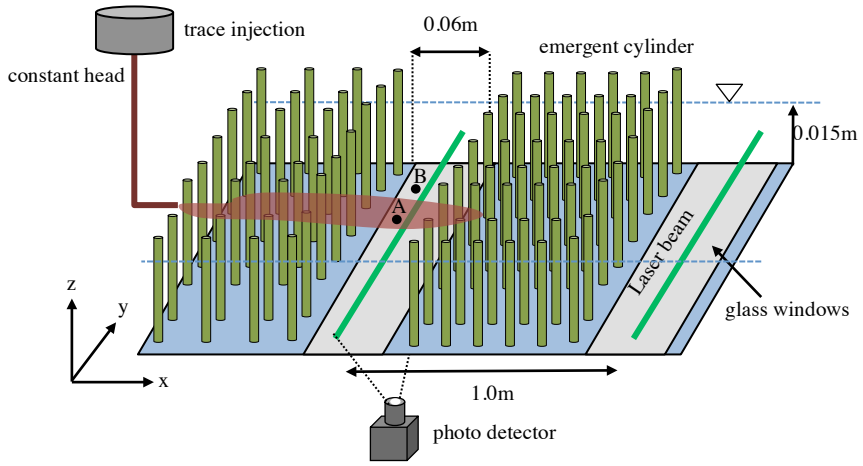

Fig. 4. Schematic diagram of emergent, full-cross-sectional vegetation with LIF windows. Note that the cylinder diameter and density are not to scale.

Rhodamine 6G was injected from a point source using a copper pipe connected to a constant head tank. Pulse injections, of 10s duration, were made to observe mixing both longitudinally and transversely. Ten repeat pulse injections were made to acquire an average distribution. Camera images were recorded at 5 Hz providing ample temporal resolution. Velocity was recorded at 50 Hz for 3 minutes using a *3D Nortek Vectrino* UVP at ten transverse locations. The channel mean velocity was then calculated from the average of the temporal mean values

from ten transverse locations. In spatially homogeneous vegetation this is deemed appropriate.

3 Results

3.1 Point probe Fluorometry

The average longitudinal concentration profile measured with the *Cyclops* fluorometers, for the 6.4 l/s discharge, injection is shown in Fig. 5a. The corresponding tests for the lateral deviation in downstream fluorometer location both positively and negatively are given in Fig. 5b and Fig. 5c, respectively. Profiles were averaged at a fixed time relative to the automated injection time for all 20 repeat injections.

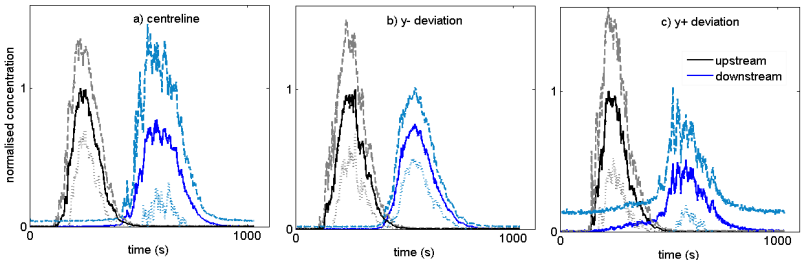

Fig. 5 Longitudinal concentration profiles for the vegetation pulse point injection are given for **a)** centreline detection and **b)** *y*- **c)** *y*+ downstream deviation. Plus or minus 1 standard deviation is shown with the dashed and dotted lines. Each profile is the average of 20 repeat tests.

Fig. 5 shows an increase in the downstream profile peak concentration when the downstream fluorometer is translated negatively in the *y* direction i.e. further from the effect of the shear layer (Fig. 5b). Conversely, downstream profile concentration reduces when the fluorometer is translated positively in the *y* direction (Fig. 5c). The progression in mass-loss at the downstream site from 5b to 5a to 5c gives the illusion that the trace is transported deeper within the vegetation; whereas the increased mixing due to shear layer turbulence diffuses the trace closer to the interface thus reducing the concentration more rapidly.

The point detection results in Fig. 5 were obtained from three independent tests to minimise flow disruption by the physical presence of multiple probes. The difference in concentration distribution between the three downstream profiles (e.g. for the centerline, positive *y* and negative *y*) indicates that the flow field in the test was not spatially homogeneous. Poor initial mixing did not lead to a cross-sectionally, well-mixed tracer (Fig. 6a) resulting in noisy data. The physical obstruction of the fluorometers was seen to direct the flow around the device (Fig. 6b). This was particularly noticeable in the point source injection tests. The small-scale tracer plume was observed to travel around the flurometer. Fig. 6b shows how the plume meander from site 1 to 2 could result in a mass imbalance between the two profiles as site 2 may detect only the edge of the plume.

Further, the small spread in tracer plume, particularly in the lower velocities, is comparable in diameter to the fluorometer probes (≈ 0.003 m). This makes the correct positioning of equipment challenging (Fig. 6c). The combination of stream-tube meandering and comparably small plume diameter can lead to the collection of unrepresentative data. It is expected that the transverse mixing and longitudinal dispersion coefficients will be functions of lateral distance across the flow – with mixing peaking in the turbulent shear layer (Ghisalberti and Nepf, 2005). Spatially extensive detection sites across the flow would therefore be required to observe and quantify mixing in vegetated shear flows. However, given the local effect on flow and tracer propagation, positioning a number of in situ fluorometers across the flow would obstruct the flow and result in secondary circulations at a comparable scale to that of the vegetation elements. Therefore point detection is not suitable for quantifying mixing in spatially variable flow fields.

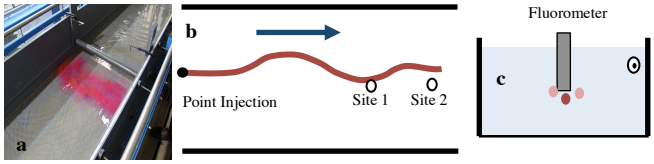

Fig. 6 **a)** An example of poor mixing and tracer "clouding". **b)** Stream-tube meander around the fluorometer **c)** Positioning error and difficulties using single-point detection probes.

3.2 LIF

An example of a two-dimensional (y,t) concentration distribution for a single pulse injection is given in Fig. 7. Upstream and downstream distributions are plotted on the same figure for time from injection against transverse location. The colour in Fig. 7 denotes concentration in ppb. Employing LIF to produce the 2D distribution is very successful. The use of a camera detection system provides high spatial resolution of up to 1280 pixels. The plot has been calibrated taking into account the dependence of laser attenuation on trace concentration as described in the preceding section. The frequent image rate (5 Hz) provides insightful imaging of the trace evolution; showing detailed turbulent structures.

A two-dimensional routing procedure was undertaken to analyse the concentration distributions given in Fig 7. The upstream distribution is broken into discretized elements of concentration. The advection and dispersion of these elements is then modelled as Gaussian using the ADE. By varying the input values of longitudinal dispersion coefficient, transverse mixing coefficient and mean, stream-wise and transverse velocity, a prediction of the downstream distribution is optimized such that the error between prediction and measurement is minimized. Optimization in this manner is applied to the full two-dimensional array of data. This differs from many previous optimized routing techniques that have generally been applied to one-dimensional data (e.g. $C = f(t)$).

An example routing optimization is shown in Fig. 8. The downstream measured profile is compared to the prediction (solid white lines in Fig. 8) made by routing the upstream measurement to that downstream.

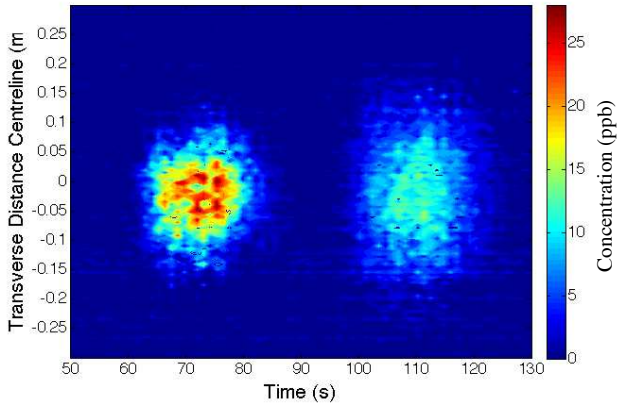

Fig. 7 Contour plots of concentration measured using the LIF system for 1.8 l/s emergent vegetation.

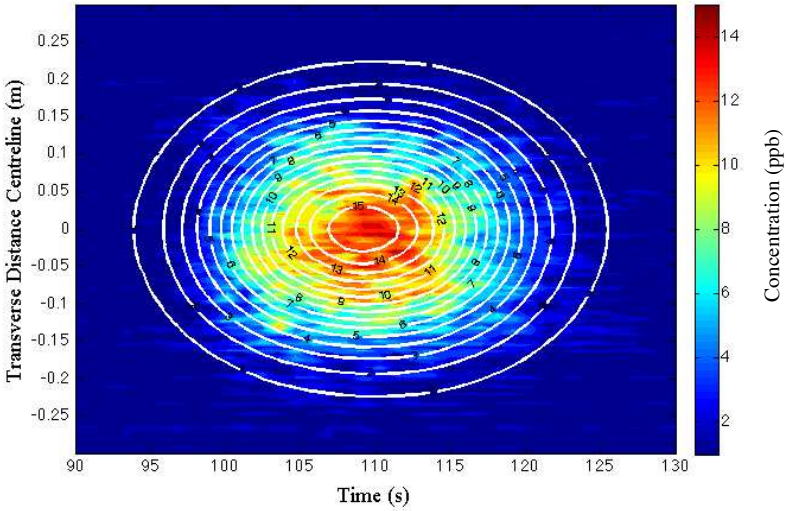

Fig. 8 2D routing prediction overlaid onto the downstream measured 2D concentration distribution.

4 Discussion

The optimization procedure assumes a spatially constant value of longitudinal dispersion and transverse mixing coefficient as well as mean longitudinal and transverse velocities. This is assumed to be a valid assumption for the present spatially homogeneous, fully vegetated test case. Fig. 8 shows a successful fit between

routed prediction and downstream observation. The approximate spread of the trace, in both y and t, is predicted. Further, the prediction is made from only one pulse measurement; predictions made using the average distribution of all 10 x repeats will provide a stronger fit. The 2D routing procedure is successful. Table 1 presents the optimized parameters from the 2D routing procedure. The average, depth mean velocity for each discharge case is compared to that predicted from profile travel time using the routing procedure. The measured and predicted velocities are comparable. However, velocity predicted based on the profile travel time over-predicts that measured using UVP. Note that the UVP measurements are the transverse average, depth-mean velocity. Calculating velocity from the mean travel time is more representative of the speed that the tracer experiences. Longitudinal Dispersion Coefficient and Transverse Mixing Coefficient are given for the three discharges. Longitudinal dispersion becomes more dominant at the higher velocity. The optimized Transverse Mixing Coefficients are compared to prediction made using Eq. 2 (Lightbody and Nepf, 2006). Predicted values are of the same order of magnitude as the measurements although consistently lower in each case. It is not yet known what the under-prediction is attributed to.

Table 1. Measured UVP velocities and mean optimized parameters for 10x repeats from the two-dimensional LIF.

Q (l/s)	u measured (m/s)	u travel time (m/s)	D_x (m^2/s) x10^{-5}	D_y (m^2/s) x10^{-5}	Fit (R^2)	D_y (m^2/s) x10^{-5} Predict Eq. 3
1.8	0.010	0.013 ± 0.00015	8.66 ± 16.7%	2.42 ± 7.4%	0.90 ± 0.01	0.88
2.4	0.013	0.017 ± 0.00016	17.0 ± 51.3%	2.97 ± 18.7%	0.84 ± 0.02	1.12
3.6	0.020	0.026 ± 0.00007	19.0 ± 11.1%	4.22 ± 2.5%	0.91 ± 0.02	1.77

5 Conclusion

Dye tracer studies were conducted in artificial vegetation to develop an accurate fluorometry detection system. In spatially heterogeneous vegetated wetlands, the mixing properties vary with location within the flow. It is therefore a necessity that any fluorometry detection has the ability to record at a range of channel locations. Employing a number of point detection fluorometers is inappropriate; resulting in unwanted flow deviation and poor spatial resolution.

A two dimensional Laser Induced Fluorometry system was developed and tested on a spatially homogeneous array of emergent cylinders. LIF provides greater spatial resolution and being non-intrusive yields more reliable data. Finally, a two-dimensional routing procedure provides estimates of the mean longitudinal and transverse velocities and the longitudinal dispersion and transverse mixing coefficients by routing the upstream and downstream, two dimensional concentration distributions.

References

Boxall, J. B. 2000. Dispersion of solutes in sinuous open channel flows. Ph,D. Thesis, University of Sheffield, UK.

Boxall, J. B. & Guymer, I. 2003. Analysis and prediction of transverse mixing coefficients in natural channels. Journal of Hydraulic Engineering-Asce, 129(2), 129-139.

Boxall, J. B. & Guymer, I. 2007. Longitudinal mixing in meandering channels: New experimental data set and verification of a predictive technique. Water Research, 41, 341-354.

Burba, G. G., Verma, S. B., Kim, J. 1999. Energy fluxes of an open water area in mid-latitude Prairie wetland. Boundary Layer Metrology. 91, 495-504.

Deng, Z. Q., Singh, V. P. & Bengtsson, L. 2001. Longitudinal dispersion coefficient in straight rivers. Journal of Hydraulic Engineering-Asce, 127 (11), 919-927.

Dixon, K., & Florian, J. 1993. Modeling mobility and effects of contaminants in wetlands,Environ. Toxicology Chem.,12, 2281-2292.

Edgar, G. J. 1990. The influence of plant structure on the species richness, biomass and secondary production of macrofaunal assemblages associated with Western Austrailian seagrass beds, J, Exp. Mar. Biol. Ecol. 137, 215-240.

Ghisalberti, M. & Nepf, H. M. 2002. Mixing layer and coherent structures in vegetated aquatic flow. J. Geophys. Res., 107 (C2), 1-11.

Ghisalberti, M. & Nepf, H.M. 2004. The limited growth of vegetated shear layers. Water Resources Research. Vol. 40 (7)

Ghisalberti, M. & Nepf, H.M. 2005. Mass transport in vegetated shear flows. Environmental Fluid Mechanics. 5 (6), 527-551.

Hart, J. R., Tiev, V., Stovin, V. R., Lacoursiere, J. O., & Guymer, I. 2014. The effects of vegetation on the hydraulic residence time of stormwater ponds. Proceedings of the 19th IAHR-APD Congress 2014, Hanoi, Vietnam.

Kadlec, R. H. & Knight, R. L. 1996. Treatment Wetlands. Lewis Publishers, Boca Raton, FL.

Kadlec, R. H. & Wallace, S. D. 2009. Treatment Wetlands – Second Edition. CRC Press.

Kashefipour, S. M. & Falconer, R. A. 2002. Longitudinal dispersion coefficients in natural channels. Water Research, 36 (7), 1854-1868.

Lightbody, A. F. & Nepf, H. M. 2006. Prediction of near-field shear dispersion in an emergent canopy with heterogeneous morphology. Environmental Fluid Mechanics, 6, 477-488.

Murphy, E., Ghisalberti, M., & Nepf, H. 2007. Model and laboratory study of dispersion in flows with submerged vegetation. Water Resource Research, Vol. 43.

National Audit Office & Environment Agency. 2010. Tckling Diffuse Water Pollution in England. Online.

Nepf, H. M., Sullivan, J. A., and Zavistoski, R. A. 1997. A model for diffusion within emergent plant canopy. Limnol. Oceanogr. 42(8), 85-95.

Nepf, H. M. 1999. Drag, turbulence, and diffusion in flow through emergent vegetation. Water Resources Research, 35 (3), 479-489.

Nepf, H. M., Ghisalberti, M., White, B. & Murphy, E. 2007. Retention time and dispersion associated with submerged aquatic canopies. Water Resource Research, Vol. 43(5), 1-10.

Nepf, H. M. & Vivoni, E. R. 2002. Flow structure in depth-limited, vegetated flow. J. Geophys. Res., 105(C12), 319-327.

Nixon, S. 1980. Between coastal marsh and coastal waters – A review of twenty years of speculation and research on the role of salt marshes in estuarine productivity and water chemistry. Estuarine and Wetland processes. 438-525.

Rominger, J. T., and Nepf, H. M. 2011. Flow adjustment and interior flow associated with a rectngular porous obstruction. J. Fluid Mechanics, vol 680, 636-659.

Serra. T, Fernando. H. J. S., & Rodriguez. R. V. 2004. Effects of emergent vegetation on lateral diffusion in wetlands. Water Research, 38, 139-147.

Shucksmith, J. D., Boxall, J. B. & Guymer, I. 2011. Determining longitudinal dispersion coefficients for submerged vegetated flow. Water Resources Research, 47(10), 503-516.

Tamura, H., Kiya, M., Arie, M. 1980. Vortex shedding from circular cylinder in moderate-Reynolds number shear flows. J Fluid Mech. 141, 721-35.

Taylor, D. S., Nixon, S., Granger, S. & Buckley, B. 1995. Nutrient limitation and the eutrophication of coastal lagoons. Mar. Ecol. Prog. Ser. 127, 235-244.

White, B. L. & Nepf, H. M. 2007. A vortex based model of velocity and shear stress in a partially vegetated shallow channel. Water Resource Research. Vol. 44.